Calculated optimized structures and hyperfine coupling constants of some radical adducts of α-phenyl-N-tert-buthyl nitrone in water and benzene solutions

ARTICLE *in* JOURNAL OF ORGANOMETALLIC CHEMISTRY · JUNE 2014

Impact Factor: 2.17 · DOI: 10.1016/j.jorganchem.2014.02.011

2 AUTHORS:

Fatih Ucun
T.C. Süleyman Demirel Üniversitesi
67 PUBLICATIONS **298** CITATIONS
SEE PROFILE

Sinem Gürkan Aydın
T.C. Süleyman Demirel Üniversitesi
2 PUBLICATIONS **1** CITATION
SEE PROFILE

Journal of Organometallic Chemistry 759 (2014) 27–32

Contents lists available at ScienceDirect

Journal of Organometallic Chemistry

journal homepage: www.elsevier.com/locate/jorganchem

Calculated optimized structures and hyperfine coupling constants of some radical adducts of α-phenyl-*N*-tert-buthyl nitrone in water and benzene solutions

Fatih Ucun*, Sinem Gürkan Aydın

Department of Physics, Faculty of Arts and Sciences, Süleyman Demirel University, Isparta, Turkey

ARTICLE INFO

Article history:
Received 27 August 2013
Received in revised form
30 January 2014
Accepted 19 February 2014

Keywords:
Hyperfine constant
Radical
EPR
DFT
HF

ABSTRACT

The ground state optimized structures of some radical adducts of α-phenyl-*N*-tert-buthyl nitrone (PBN) in water and benzene solutions were calculated by using DFT (B3LYP, B3PW91 and PBEPBE) and HF methods with 6-311++G(d, p), 6-31G(d, p) and LanL2DZ levels. As trapped radicals, F, Cl, Br, H, OH, CN, NCO, and N_3 were used. The calculated isotropic hyperfine coupling constants of all the trapped radicals were seen to be in good agreement with the corresponding experimental data. The hyperfine coupling constant due to the β proton of nitroxide radical was seen to be effected with the opposite spin density of oxygen nucleus bonded to the nitrogen. From all the calculated data it was concluded that for hyperfine calculations the DFT method is superior relative to the HF method. Also the geometrical parameters for the ground state optimized structures of all the radical adducts were listed, and the binding energies of all the trapped radicals were obtained.

1. Introduction

Electron paramagnetic resonance (EPR) is a sophisticated spectroscopic technique that detects free radicals or inorganic complexes in chemical and biological systems. Unfortunately the lifetimes of most radicals generated with chemical reaction, irradiation or some other methods are short to be detected by EPR. So, the spin trapping method is used to increase of their lifetimes, and to detect them. There are two kinds of spin traps; nitrose and nitrone compounds. In nitrose compounds such as MNP (2-methyl-2-nitrosopropone) the radicals are trapped directly to the nitrose nitrogen while in nitrone compounds such as (PBN) α-phenyl-*N*-tert-butyl nitrone they are trapped to carbon adjacent to the nitrogen [1].

The characteristic feature of trapped radical by PBN is the triplet and doublet hyperfine splitting due to the N nucleus and β hydrogen nucleus, respectively. Hyperfine coupling constants of some spin adducts are tabulated in Ref. [1]. Typical PBH–OH spin adduct has $a_N = 14.66$ G and $a_H^\beta = 3.1$ G characteristic features. The hyperfine coupling constant (hfcc) due to the β proton of nitroxide radical can be obtained by the relation $a_\beta = B_0 + B_1\cos^2\theta$ [2]. Where B_0 is the spin polarization contribution (0–3.5) and B_1 the hyperconjugative contribution (~50), and θ is the angle between the P_z orbital of the nitrogen and the projection of the CH bond to the P_z orbital plane.

The isotropic hfcc's are very sensitive to the spin density at nucleus position, so, are very difficult to compute in a quantitative agreement with the experimental data [3]. The correlation of radical structure with spin adducts parameters was studied by Lawrence and et al. [4]. The hyperfine parameters of some radicals were studied by using the density function theory (DFT) and configuration-interaction (CI) methods [5]. Some authors have calculated the g-tensors of some organic radicals by Hartree–Fock (HF) method [6]. EPR parameters (*g* and *a* tensors) of sulfur centered radicals have been calculated using multi-configurationally self consistent field (MCSCF) response and DFT/B3LYP methods [7].

Since only a few hfcc's of trapped radicals can be observed by EPR, the determination of structures of radical adducts is difficult. Therefore, theoretical calculations should be used for this. The calculation of hfcc's of all nuclei in a radical structure, some being agreement with the experimental data, may contribute to interpret the properties of radical. These calculations may also yield to further knowledge about the other properties (spin density, bond length, bond angle, binding energy of radical, i.e.) being difficult to observe, experimentally. So, in this study, the optimized structures

* Corresponding author. Fax: +90 246 237 1106.
E-mail address: fatihucun@sdu.edu.tr (F. Ucun).

http://dx.doi.org/10.1016/j.jorganchem.2014.02.011
0022-328X/

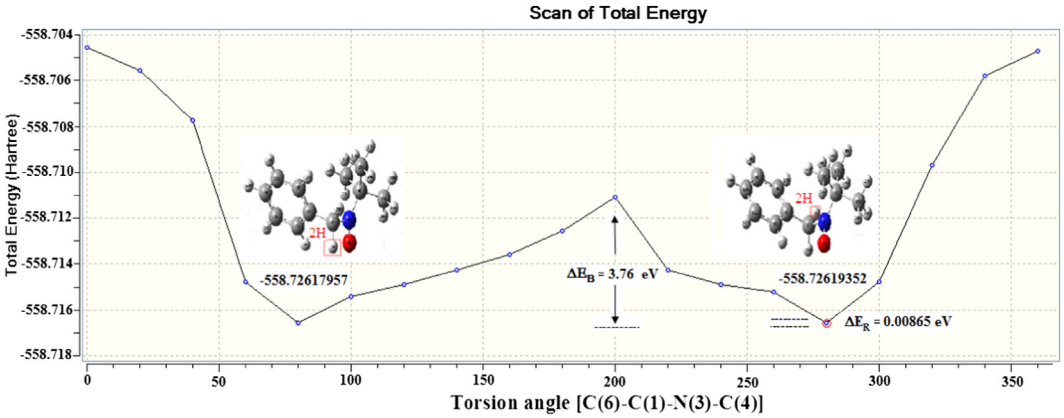

Fig. 1. PES graph of PBN–H spin adduct.

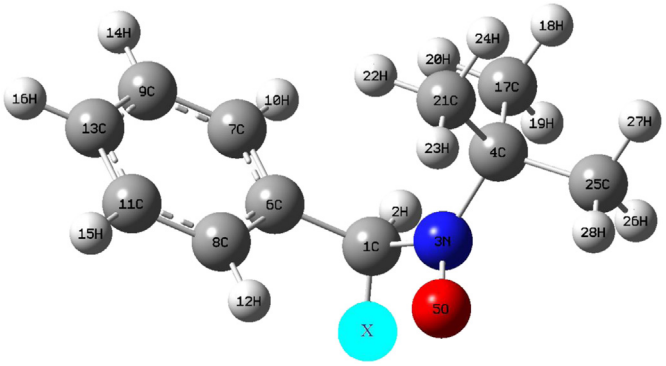

Fig. 2. Optimized structures of PBN–X spin adducts (X; F, Cl, Br, H, OH, CN, NCO, N_3).

and hyperfine coupling constants of some radical adducts of PBN were calculated by using DFT(B3LYP, B3PW91 and PBEPBE) and HF methods with 6-311++G(d, p), 6-31G(d, p) and LanL2DZ levels. The calculated results were compared with the experimental data. The binding energies of all the trapped radicals were also determined.

2. Computational details

The structures of radical adducts of PBN were optimized in water and benzene solutions by using spin-unrestricted DFT(B3LYP, B3PW91 and PBEPBE) and HF methods with 6-311++G(d, p), 6-31G(d, p) and LanL2DZ basis sets implemented in the polarizable continuum model (PCM) [8,9]. All calculations were performed using Gaussian 03 package [10] and Gauss-View molecular visualization programs [11] on the personal computer. In the calculations

Table 1
Some selected geometrical parameters of PBN–X radical product calculated at DFT(B3LYP) 6-311++G(d, p) level in water and benzene solutions.

	PBN–X							
	Benzene					Water		
	F	Cl	Br	H	CN	OH	N3	NCO
Dihedral angle (°)								
C(17)–C(4)–N(3)–C(1)	−141.5	14.0	−15.2	−26.1	26.2	−25.7	140.0	45.9
C(25)–C(4)–N(3)–C(1)	−21.0	−107.3	106.3	−142.4	−95.5	145.1	−101.3	−75.2
C(21)–C(4)–N(3)–C(1)	99.9	134.0	−135.0	95.2	145.6	95.7	19.7	165.2
C(4)–N(3)–C(1)–C(6)	71.8	−153.7	63.2	−78.9	−148.6	−81.1	−68.6	−105.8
O(5)–N(3)–C(1)–H(2)	−2.3	164.5	−11.9	−151.3	171.2	−159.3	11.3	−150.5
O(5)-N(3)-C(1)-X	111.0	−84.9	96.3	−36.0	73.0	−45.2	−105.4	−34.4
N(3)–C(1)–C(6)–C(7)	46.6	114.9	128.0	120.8	96.7	125.4	−49.9	131.4
N(3)–C(1)–C(6)–C(8)	−137.6	−64.9	55.2	−60.4	−81.9	−56.4	133.7	−49.8
Angle (°)								
H(20)–C(17)–C(4)	112.3	112.1	112.5	112.4	111.8	112.4	110.8	111.2
H(26)–C(25)–C(4)	110.9	111.1	110.8	110.8	111.5	110.8	109.4	109.6
H(22)–C(21)–C(4)	110.9	111.0	111.2	111.2	110.9	111.3	112.2	111.0
C(4)–N(3)–O(5)	117.0	116.6	115.4	117.4	117.3	117.6	116.5	119.8
O(5)–N(3)–C(1)	115.5	118.7	113.9	116.5	116.1	115.8	115.0	116.8
H(2)–C(1)–N(3)	104.2	109.2	104.3	109.1	107.6	107.5	102.8	107.8
X–C(1)–C(6)	110.1	109.7	114.1	110.4	112.5	113.16	110.5	111.5
C(7)–C(6)–C(1)	119.0	117.7	115.6	120.3	118.7	119.0	118.2	119.0
C(1)–C(6)–C(8)	121.3	122.9	125.3	120.8	121.6	121.8	122.3	121.4
Bond length (Å)								
H(20)–C(17)	1.090	1.093	1.082	1.091	1.094	1.092	1.092	1.092
H(28)–C(25)	1.090	1.091	1.082	1.089	1.091	1.090	1.092	1.092
H(22)–C(21)	1.091	1.093	1.084	1.091	1.092	1.092	1.090	1.092
C(25)–C(4)	1.536	1.539	1.533	1.536	1.539	1.537	1.540	1.540
C(4)–N(3)	1.513	1.518	1.500	1.506	1.515	1.507	1.515	1.509
N(3)–O(5)	1.283	1.273	1.259	1.284	1.273	1.281	1.284	1.275
N(3)–C(1)	1.460	1.439	1.440	1.478	1.497	1.496	1.485	1.494
C(1)–H(2)	1.091	1.082	1.075	1.089	1.089	1.088	1.096	1.091

Table 1 (*continued*)

	PBN–X							
	Benzene					Water		
	F	Cl	Br	H	CN	OH	N3	NCO
C(1)–X	1.409	1.908	1.998	1.092	1.474 N–C 1.153	1.406 O–H 0.981	1.485 N–N 1.230 N–N 1.132	1.448 N–C 1.209 C–O 1.172
C(1)–C(6)	1.515	1.502	1.522	1.520	1.521	1.523	1.520	1.525
C(6)–C(7)	1.398	1.398	1.394	1.398	1.397	1.398	1.400	1.396
C(7)–H(10)	1.085	1.086	1.076	1.088	1.086	1.088	1.087	1.088
C(8)–H(12)	1.083	1.082	1.072	1.086	1.084	1.086	1.084	1.085
X···O(5)	3.221	3.364	3.600	2.428	2.976	2.692	3.272	2.677

Table 2
Hfcc's and energies for the ground state optimized structures of PBN–X radical products in benzene solution, and the binding energies of the radicals.

			Hyperfine coupling constants (Gauss)					Energy (Hartree/particle)	Binding energy of radical/ BSSE corrected (kcal/mol)
			C(1)	H(2)	N(3)	O(5)	X		
PBN–F	Exp. [1]			1.18	12.20		45.60 ^{19}F		
	DFT/B3LYP	6-311G++(d, p)	−0.95	0.39	8.24	−10.85	43.99	−658.142907	95.10
		6-31G(d, p)	0.24	0.88	12.06	−16.99	32.07	−657.975623	97.09
		LanL2DZ	−0.49	0.21	13.67	−29.48	42.51	−657.891446	86.77
	DFT/B3PW91	6-311G++(d, p)	−0.86	0.31	6.96	−7.21	43.50	−657.883545	95.35
		6-31G (d, p)	0.11	0.69	11.42	−15.98	34.53	−657.729545	96.75
		LanL2DZ	−0.77	0.20	13.05	−28.26	42.73	−657.648068	86.62
	DFT/PBEPBE	6-311G++(d, p)	1.63	0.00	5.99	−4.27	53.63	−657.330988	94.24
		6-31G (d, p)	2.74	0.45	10.05	−11.60	41.08	−657.164240	95.54
		LanL2DZ	2.59	−0.20	11.18	−21.71	55.28	−657.101930	85.98
	HF	6-311G++(d, p)	−7.47	0.95	17.22	−41.43	28.90	−654.138840	95.07
		6-31G (d, p)	−5.46	0.98	18.30	−41.01	22.14	−653.997454	98.19
		LanL2DZ	−6.30	0.74	16.63	−65.00	22.28	−653.830237	89.15
PBN–Cl	Exp. [1]			0.75	12.12		6.05, 4.88 ^{35}Cl , ^{37}Cl		
	DFT/B3LYP	6-311G++(d, p)	5.64	1.27	6.92	−10.07	7.53	−1018.497534	49.67
		6-31G (d, p)	5.72	0,66	9.71	−16.54	7.60	−1018.335699	49.97
		LanL2DZ	3.86	1.49	10.18	−28.01	0.00	−572.988042	38.94
	DFT/B3PW91	6-311G++(d, p)	5.16	1.11	6.00	−6.51	7.22	−1018.223723	53.53
		6-31G (d, p)	5.20	0.63	9.57	−15.55	7.39	−1018.073782	53.63
		LanL2DZ	3.66	1.47	10.11	−26.83	0.00	−572.806604	42.44
	DFT/PBEPBE	6-311G++(d, p)	10.68	1.02	4.54	−3.58	9.57	−1017.580815	50.02
		6-31G (d, p)	11.36	0.39	7.48	−10.71	9.93	−1017.423360	49.69
		LanL2DZ	10.20	0.96	7.50	−19.32	0.00	−572.286607	38.39
	HF	6-311G++(d, p)	−5.80	1.15	15.29	−40.88	3.26	−1014.177048	62.88
		6-31G (d, p)	−5.38	0.74	16.16	−41.56	3.20	−1014.037652	64.03
		LanL2DZ	−6.62	0.72	12.56	−65.14	0.00	−569.087780	56.86
PBN–Br	Exp. [1]				11.30		32.4, 34.9 ^{79}Br, ^{81}Br		
	DFT/B3LYP	6-311G++(d, p)	3.36	0.36	7.27	−10.04	25.41	−3132.413241	46.37
		6-31G (d, p)	4.54	0.08	10.26	−16.32	33.75	−3129.846850	45.78
		LanL2DZ	1.33	0.40	11.65	−28.06	0.00	−571.199614	40.89
	DFT/B3PW91	6-311G++(d, p)	3.20	0.41	6.15	−6.52	25.72	−3132.177049	49.19
		6-31G (d, p)	4.31	0.11	9.95	−15.36	33.82	−3129.651509	48.66
		LanL2DZ	1.36	0.41	11.35	−26.88	0.00	−517.017990	44.19
	DFT/PBEPBE	6-311G++(d, p)	9.11	−0.22	4.80	−3.64	35.18	−3131.286788	48.14
		6-31G (d, p)	10.21	−0.52	8.18	−10.67	44.52	−3128.731285	45.82
		LanL2DZ	8.58	−0.44	8.81	−19.97	0.00	−570.204598	41.33
	HF	6-311G++(d, p)	−10.28	2.04	16.55	−40.53	9.97	−3127.031231	58.18
		6-31G (d, p)	−7.49	1.65	17.15	−7.57	14.84	−3124.444850	56.93
		LanL2DZ	−11.59	2.20	15.36	−64.17	0.00	−567.303052	53.51
PBN–H	Exp. [1]			7.13	14.25				
	DFT/B3LYP	6-311G++(d, p)	−5.10	4.28	10.37	−10.28	5.63	−558.875137	108.75
		6-31G(d, p)	−4.28	4.33	13.51	−15.85	5.41	−558.763620	109.41
		LanL2DZ	−5.43	4.34	16.75	−27.41	5.03	−558.644710	112.39
	DFT/B3PW91	6-311G++(d, p)	−5.47	5.23	9.16	−6.87	5.44	−558.663414	108.97
		6-31G (d, p)	−4.46	4.32	12.81	−14.82	5.87	−558.533151	107.85
		LanL2DZ	−5.98	4.60	16.69	−25.54	5.68	−558.445910	111.31
	DFT/PBEPBE	6-311G++(d, p)	−3.85	4.29	8.66	−3.97	5.91	−558.149620	98.55
		6-31G (d, p)	−2.72	3.44	12.57	−10.58	6.65	−558.019922	97.71
		LanL2DZ	−3.98	3.99	14.88	−19.98	5.52	−557.939155	101.11
	HF	6-311G++(d, p)	−12.24	4.97	21.18	−39.81	5.08	−555.254334	132.42
		6-31G (d, p)	−10.24	4.72	21.92	−38.65	5.22	−555.142370	133.28
		LanL2DZ	−11.60	4.83	24.50	−62.08	4.33	−554.969761	141.86

(*continued on next page*)

Table 2 (*continued*)

			Hyperfine coupling constants (Gauss)					Energy (Hartree/particle)	Binding energy of radical/ BSSE corrected (kcal/mol)
			C(1)	H(2)	N(3)	O(5)	X		
PBN–CN	Exp. [1]			1.94	14.96				
	DFT/B3LYP	6-311G++(d, p)	−0.95	0.84	10.95	−10.43	$a_C = 13.83$ $a_N = 0.33$	−651.129921	100.35
		6-31G (d, p)	−4.50	1.86	13.70	−16.39	$a_C = 5.08$ $a_N = -0.02$	−650.971793	113.73
		LanL2DZ	2.37	0.42	16.39	−28.53	$a_C = 13.52$ $a_N = 0.18$	−650.851951	101.08
	DFT/B3PW91	6-311G++(d, p)	−1.39	0.58	9.47	−6.82	$a_C = 13.63$ $a_N = 0.31$	−650.867116	102.24
		6-31G (d, p)	−4.57	2.20	13.54	−15.33	$a_C = 4.85$ $a_N = -0.02$	−650.723658	116.36
		LanL2DZ	−2.97	0.42	15.67	−27.18	$a_C = 13.86$ $a_N = 0.17$	−650.606923	102.88
	DFT/PBEPBE	6-311G++(d, p)	0.75	1.61	9.66	−4.01	$a_C = 14.39$ $a_N = 0.29$	−650.305519	93.87
		6-31G (d, p)	−3.10	1.74	12.72	−10.92	$a_C = 5.10$ $a_N = 0.00$	−650.151609	106.90
		LanL2DZ	−0.53	0.88	14.97	−20.85	$a_C = 14.73$ $a_N = 0.26$	−650.051753	93.60
	HF	6-311G++(d, p)	−12.35	2.40	19.28	−40.64	$a_C = 7.22$ $a_N = -0.47$	−646.997660	132.96
		6-31G (d, p)	−10.48	2.69	20.41	−40.16	$a_C = 7.01$ $a_N = -0.66$	−646.865473	135.59
		LanL2DZ	−12.12	2.99	21.01	−63.75	$a_C = 10.83$ $a_N = -1.94$	−646.655604	136.49

Table 3
Hfcc's and energies for the ground state optimized structures of PBN–X radical products in water solution, and the bonding energies of the radicals.

			Hyperfine coupling constants (Gauss)					Energy (Hartree/particle)	Binding energy of radical/BSSE corrected (kcal/mol)
			C(1)	H(2)	N(3)	O(5)	X		
PBN–OH	Exp. [1]			2.74	15.49		0.604 ^{1}H		
	DFT/B3LYP	6-311G++(d, p)	−5.30	3.40	10.43	−10.23	$a_O = -0.36$ $a_H = -0.29$	−634.133942	114.74
		6-31G(d, p)	−4.55	4.59	13.34	−15.68	$a_O = -0.01$ $a_H = -0.29$	−633.972416	99.46
		LanL2DZ	−5.90	5.19	17.09	−26.46	$a_O = 0.27$ $a_H = -0.30$	−633.863029	87.95
	DFT/B3PW91	6-311G++(d, p)	−5.58	5.30	8.67	−6.97	$a_O = 0.25$ $a_H = -0.34$	−633.877504	103.44
		6-31G(d, p)	−4.62	5.99	13.04	−14.84	$a_O = 0.35$ $a_H = -0.39$	−633.729583	105.79
		LanL2DZ	−6.18	5.49	16.59	−25.27	$a_O = 0.30$ $a_H = -0.32$	−633.630378	98.20
	DFT/PBEPBE	6-311G++(d, p)	−4.25	3.75	8.30	−4.11	$a_O = -0.43$ $a_H = -0.31$	−633.338542	96.45
		6-31G(d, p)	−9.15	2.99	21.44	−38.64	$a_O = -032$ $a_H = -0.53$	−629.999461	104.12
		LanL2DZ	−4.40	3.57	14.84	−19.42	$a_O = -0.39$ $a_H = -0.31$	−633.096864	91.28
	HF	6-311G++(d, p)	−13.43	4.09	22.68	−38.78	$a_O = -0.02$ $a_H = -0.44$	−630.142888	106.63
		6-31G(d, p)	−9.14	2.99	21.44	−38.64	$a_O = -0.39$ $a_H = -0.31$	−629.999461	114.08
		LanL2DZ	−12.88	3.97	26.30	−61.09	$a_O = -0.06$ $a_H = -0.23$	−629.819500	113.40
PBN–N_3	Exp. [1]			2.25	14.91		2.25 ^{14}N		
	DFT/B3LYP	6-311G++(d, p)	−2.25	0.30	9.82	−10.39	$a_N = 3.43$ $a_N = -0.16$ $a_N = 0.19$	−722.505679	76.11
		6-31G(d, p)	−0.77	0.24	12.99	−16.28	$a_N = 2.80$ $a_N = -0.14$ $a_N = 0.32$	−722.323286	56.54
		LanL2DZ	−3.59	0.47	15.79	−27.75	$a_N = 2.87$ $a_N = -0.21$ $a_N = 0.55$	−722.183997	55.87
	DFT/B3PW91	6-311G++(d, p)	−2.06	0.30	8.38	−7.03	$a_N = 3.60$ $a_N = -0.13$ $a_N = 0.10$	−722.214941	59.13
		6-31G(d, p)	−0.76	0.27	12.44	−15.28	$a_N = 2.99$ $a_N = -0.14$ $a_N = 0.32$	−722.050131	58.29
		LanL2DZ	−3.69	0.47	15.04	−26.81	$a_N = 3.04$ $a_N = -0.18$ $a_N = 0.52$	−721.909066	58.02
	DFT/PBEPBE	6-311G++(d, p)	0.85	0.14	7.79	−4.09	$a_N = 4.13$ $a_N = -0.12$ $a_N = 0.11$	−721.631040	55.09
		6-31G(d, p)	2.05	0.02	11.20	−10.70	$a_N = 3.75$ $a_N = -0.04$ $a_N = 0.35$	−721.458236	47.59
		LanL2DZ	−0.29	0.20	13.24	−20.15	$a_N = 3.81$ $a_N = -0.08$ $a_N = 0.67$	−721.336752	53.43
	HF	6-311G++(d, p)	−11.35	1.36	21.09	−40.09	$a_N = 2.26$ $a_N = -0.72$ $a_N = 0.42$	−717.973443	70.75
		6-31G(d, p)	−9.07	1.22	21.62	−39.49	$a_N = 1.43$ $a_N = -0.77$ $a_N = 0.58$	−717.820772	70.06
		LanL2DZ	−11.71	1.80	23.75	−62.89	$a_N = 2.26$ $a_N = -0.57$ $a_N = 0.10$	−717.566766	71.22
PBN–NCO	Exp. [1]			3.21	15.91		1.89 ^{14}N		
	DFT/B3LYP	6-311G++(d, p)	−2.92	4.35	10.63	−10.15	$a_N = 0.55$ $a_C = -0.22$ $a_O = -0.25$	−726.410709	88.45
		6-31G(d, p)	−2.05	3.78	14.12	−15.90	$a_N = 0.60$ $a_C = -0.13$ $a_O = -0.39$	−726.222990	93.05
		LanL2DZ	−3.77	2.75	16.78	−26.97	$a_N = 1.39$ $a_C = 0.24$ $a_O = -0.39$	−726.096178	85.65
	DFT/B3PW91	6-311G++(d, p)	−3.12	4.05	9.04	−6.93	$a_N = 0.60$ $a_C = -0.28$ $a_O = -0.20$	−726.117320	59.13
		6-31G(d, p)	−2.76	5.56	13.93	−14.89	$a_N = 0.30$ $a_C = -0.11$ $a_O = -0.31$	−725.952099	93.39
		LanL2DZ	−3.92	2.58	16.17	−25.84	$a_N = 1.47$ $a_C = 0.24$ $a_O = -0.40$	−725.819047	88.06
	DFT/PBEPBE	6-311G++(d, p)	−0.94	4.25	8.77	−4.10	$a_N = 0.46$ $a_C = -0.19$ $a_O = -0.26$	−725.516742	90.96
		6-31G(d, p)	−0.64	5.83	13.36	−10.62	$a_N = 0.16$ $a_C = 0.20$ $a_O = -0.38$	−725.339295	90.39
		LanL2DZ	−2.07	4.00	15.21	−19.11	$a_N = 0.76$ $a_C = 0.18$ $a_O = -0.53$	−725.233854	85.65
	HF	6-311G++(d, p)	−12.54	4.80	22.87	−38.88	$a_N = 0.84$ $a_C = -0.37$ $a_O = -0.40$	−721.908681	102.37
		6-31G(d, p)	−10.08	4.59	24.09	−38.99	$a_N = 0.75$ $a_C = -0.25$ $a_O = -0.42$	−721.747161	102.38
		LanL2DZ	−7.31	0.37	21.46	−64.36	$a_N = 3.96$ $a_C = 1.04$ $a_O = 0.45$	−721.511022	87.80

Table 4
Correlation coefficients (R^2) estimated for the linear regressions between the experimental and calculated hfcc's of all the considered radical products.

Method	Basis set	R^2
DFT/B3LYP	6-311G++(d, p)	0.9554
	6-31G(d, p)	0.9412
	LanL2DZ	0.9754
DFT/B3PW91	6-311G++(d, p)	0.9254
	6-31G (d, p)	0.9509
	LanL2DZ	0.9791
DFT/PBEPBE	6-311G++(d, p)	0.8867
	6-31G (d, p)	0.8871
	LanL2DZ	0.9691
HF	6-311G++(d, p)	0.5841
	6-31G (d, p)	0.5396
	LanL2DZ	0.5693

the molecular structure was firstly taken with a torsion angle C(6)–C(1)–N(3)–C(4) which we have designed as a characteristic angle for these structures, and scanned around this angle from 0° to 360° at increments of 20° by using DFT/B3LYP 6-31 G(d) method. Potential Energy Surface (PES) scans of the radical adducts of PBN showed one or two minimum-energy structures. These minimum structures were chosen to obtain the further optimized ones. As an example, the PES graph of PBN–H spin adduct are given in Fig. 1. The graph shows two minimum energy structures with a relative energy of 0.0086 eV and a barrier energy of 3.76 eV between them. The binding energies of all the trapped radicals were calculated using supramolecular approach corrected for basis set superposition error (BSSE) according to Boys counterpoise method [12] at the optimized levels. Natural bond orbital (NBO) analysis [13–15] has been performed to evaluate natural population analysis (NPA) charges at the B3LYP/6-311++G(d, p) level of theory.

3. Results and discussion

The calculated ground state optimized structures of the radical adducts of PBN are shown in Fig. 2. The some selected geometrical parameters (bond length, bond angle and torsion angle) calculated at the B3LYP/6-311++G(d, p) level of theory in water and benzene solutions are given in Table 1, in accordance with the atom numberings in Fig. 2. As seen from the table there are slight differences between them. As we expect that while the electronegativity of halogen trapped by PBN decreases the distance C(1)–X increases, and this causes some relative geometrical differences. In addition the bond length O···X for the radical product with the most

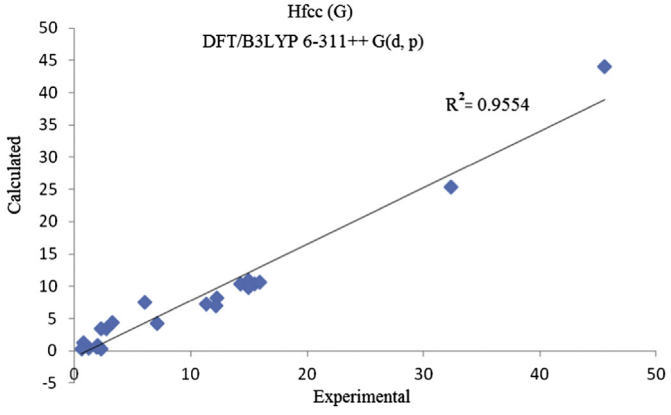

Fig. 3. Correlation graph between the calculated and experimental hfcc's of all the considered radical products (B3LYP/6-311++G(d, p)).

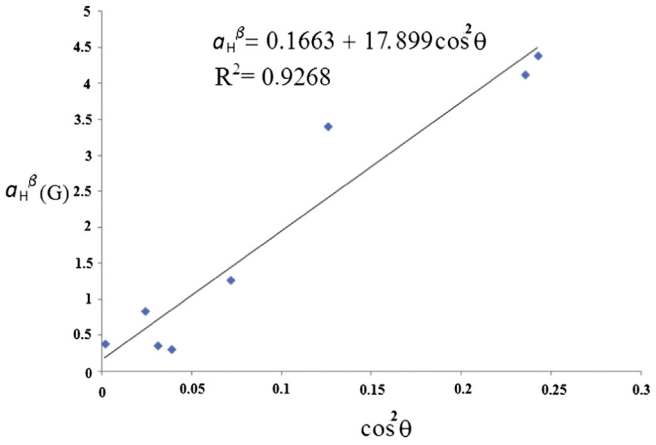

Fig. 4. Varying graph of the hfcc's due to the β proton of the nitroxide radical with angle between the P_z orbital of the nitrogen and the projection of the CH bond to the P_z orbital plane.

electronegative atom F is the shortest (3.221 Å) but, is the longest (3.600 Å) for the one with the least electronegative atom Br depending on the atomic radius of the halogen atom.

The hfcc's and energies for the ground state optimized structures of PBN–X radical products in water and benzene solutions are tabulated in Tables 2 and 3. For comparison the experimental hfcc's are also given in the tables [1]. Taking into account that the calculated results based on a single molecule may not match to the experimental one in which multiple interactions takes place, there is reasonable agreement between the calculated and experimental values. To show the interrelation the correlation coefficients (R^2) between the experimental and calculated hfcc's of all the considered radical products were obtained and given in Table 4. As an example the correlation graph between the experimental and calculated (B3LYP/6-311++G(d, p)) values is given in Fig. 3. From the R^2 values in Table 4 it can be concluded that for hyperfine calculations the DFT method is superior relative to the HF method, and in addition, that the DFT/B3LYP/6-311++G(d, p) level of theory is generally more suitable than the others since the LanL2DZ basis set gives zero for hfcc's of heavy atoms (see Table 2). In Tables 2 and 3 are also given the binding energies of all the trapped radicals by PBN calculated at the optimized levels. As seen the most tight-binding radical between the trapped halogens is the F radical.

The variation of the hfcc's due to the β proton (H(2)) of the nitroxide radical (N(3)) with the angle θ between the P_z orbital of the nitrogen and the projection of the CH bond to the P_z orbital plane is found as $a_\beta = 0.1663 + 17.899\cos^2\theta$ (Fig. 4). In here we used together the hfcc's of the β protons calculated in the different solutions since it was experimentally found that the hfcc due to the β proton of nitro radical anion is insensitive with solvent change [16].

Table 5
Hfcc's due to β proton of nitrogen radical and the angle between P_z orbital of nitrogen and projection of CH bond to P_z orbital plane calculated at DFT(B3LYP) 6-311++G(d, p) level.

PBN–X	θ (°)	$a^\beta_{H(2)}$
NCO	60.5	4.347
H	61.0	4.126
OH	69.3	3.404
Cl	74.5	1.269
CN	81.2	0.836
F	92.3	0.388
Br	100.1	0.364
N_3	101.3	0.305

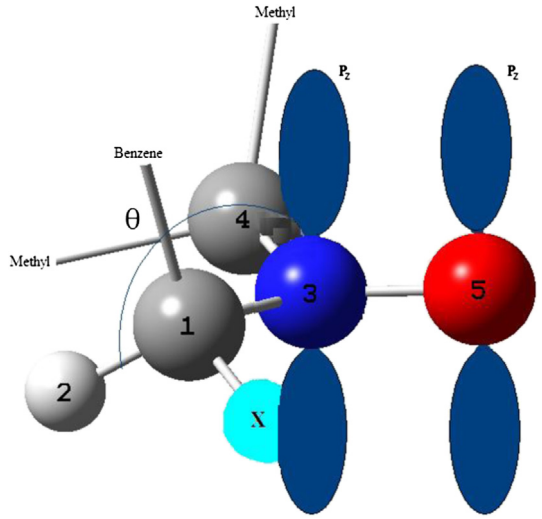

Fig. 5. Definition of the angle θ between the P_z orbital of the nitrogen and the projection of CH bond to the P_z orbital plane.

When we compare this equation with the McConnell relation of $a_\beta = B_0 + B_1\cos^2\theta$ where B_0, as we mentioned before, is the spin polarization contribution (0–3.5) and B_1 the hyperconjugative contribution ($\sim$50) [2] we see that the value of B_0 is agree, but B_1 is somewhat low. This can be attributed to the opposite spin density of the oxygen O(5) nucleus ($a_{O(5)} \sim -10$ G) bonded to the nitrogen N(3). Table 5 shows the values of the H(2) hfcc's and θ's for all the radical products. The θ's are obtained by the help of the dihedral angle of C(4)–N(3)–C(1)–H(2) (Fig. 5). In Fig. 6 the single occupied molecular orbital (SOMO) graph (such as half-filled HOMO of a radical) for the PBN–F spin adduct is given. The graph shows that the sign of the charge density on the N(3) and O(5) atoms is opposite. The NPA charges and Mulliken spin densities of the N(3) and O(5) atoms for all PBN–X spin adducts are given in Table 6. The NPA charges also show a higher negative charge on the oxygen atom and a nearly positive charge on the nitrogen atom. From

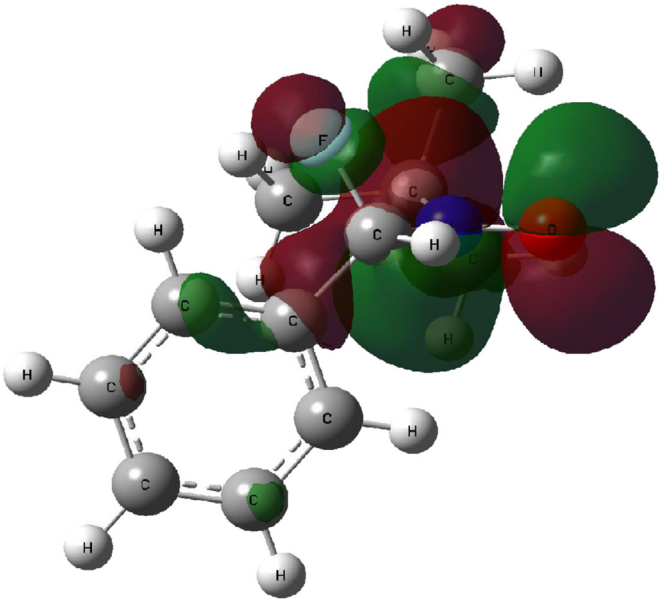

Fig. 6. SOMO plot for PBN–F spin adduct.

Table 6
Mulliken atomic spin densities and NPA charges calculated at DFT(B3LYP) 6-311++G(d, p) level.

PBN–X	Mulliken atomic spin densities		NPA atomic charges	
	O(5)	N(3)	O(5)	N(3)
H	0.471504	0.508745	−0.459	−0.012
NCO	0.473975	0.499753	−0.458	−0.002
OH	0.477403	0.498846	−0.488	−0.017
N_3	0.492666	0.488142	−0.462	0.001
Br	0.523082	0.395741	−0.410	−0.034
F	0.532917	0.447141	−0.420	−0.051
CN	0.539522	0.442649	−0.408	−0.010
Cl	0.540362	0.386205	−0.397	−0.026

Table 6 we can also say that the spin density on the N atom decreases while the one of the O atom increases, and this causes a lower hfcc for the β proton H(2).

4. Conclusions

The optimized ground state structures of some radical adducts of α-phenyl-*N*-ter-buthyl nitrone (PBN) in water and benzene solutions were determined by using DFT(B3LYP, B3PW91 and PBEPBE) and HF methods with 6-311++G(d, p), 6-31G(d, p) and LanL2DZ levels. Selected radicals are F, Cl, Br, H, CN, OH, N_3 and NCO, respectively. The calculated isotropic hyperfine coupling constants were seen to be in agreement with the experimental results. From all the calculated data it was seen that in hyperfine calculations the DFT method is better than the HF method. Also the calculated geometrical parameters (bond length, bond angle and torsion angle) for all the radical products were listed, and the binding energies of all the trapped radicals were determined. The hyperfine coupling constant due to the β proton of the nitroxide radical was found to be affected with the spin density on the oxygen nucleus bonded to the nitrogen.

References

[1] G.R. Buettner, Free Radic. Biol. Med. 3 (1987) 259–303.
[2] J.R. Morton, Chem. Rev. 64 (1964) 453–471.
[3] D. Feller, E.R. Davidson, Chem. Phys. 80 (1984) 1006–1018.
[4] D.L. Haire, U.M. Oehler, P.H. Krygsman, E.G. Janzen, J. Org. Chem. 53 (1988) 4535–4542.
[5] Bo-Z. Chen, Ming-B. Huang, Chem. Phys. Lett. 308 (1999) 256–262.
[6] M. Engström, O. Vahtras, H. Agren, Chem. Phys. 243 (1999) 263–271.
[7] M. Engström, O. Vahtras, H. Agren, Chem. Phys. Lett. 328 (2000) 483–491.
[8] S. Miertus, E. Scrocco, J. Tomasi, Chem. Phys. 55 (1981) 117–129.
[9] R. Cammi, J. Tomasi, J. Comput. Chem. 16 (1995) 1449–1458.
[10] M.J. Frisch, G.W. Trucks, H.B. Schlegel, G.E. Scuseria, M.A. Robb, J.R. Cheeseman, J.A. Montgomery Jr., T. Vreven, K.N. Kudin, J.C. Burant, J.M. Millam, S.S. Iyengar, J. Tomasi, V. Barone, B. Mennucci, M. Cossi, G. Scalmani, N. Rega, G.A. Petersson, H. Nakatsuji, M. Hada, M. Ehara, K. Toyota, R. Fukuda, J. Hasegawa, M. Ishida, T. Nakajima, Y. Honda, O. Kitao, H. Nakai, M. Klene, X. Li, J.E. Knox, H.P. Hratchian, J.B. Cross, C. Adamo, J. Jaramillo, R. Gomperts, R.E. Stratmann, O. Yazyev, A.J. Austin, R. Cammi, C. Pomelli, J.W. Ochterski, P.Y. Ayala, K. Morokuma, G.A. Voth, P. Salvador, J.J. Dannenberg, V.G. Zakrzewski, S. Dapprich, A.D. Daniels, M.C. Strain, O. Farkas, D.K. Malick, A.D. Rabuck, K. Raghavachari, J.B. Foresman, J.V. Ortiz, Q. Cui, A.G. Baboul, S. Clifford, J. Cioslowski, B.B. Stefanov, G. Liu, A. Liashenko, P. Piskorz, I. Komaromi, R.L. Martin, D.J. Fox, T. Keith, M.A. Al-Laham, C.Y. Peng, A. Nanayakkara, M. Challacombe, P.M.W. Gill, B. Johnson, W. Chen, M.W. Wong, C. Gonzalez, J.A. Pople, GAUSSIAN 03, Revision C.02, Gaussian Inc., Pittsburgh, PA, 2003.
[11] A. Frish, A.B. Nielsen, A.J. Holder, Gauss View User Manual, Gaussian Inc., Pittsburg, PA, 2001.
[12] S.F. Boys, F. Bernardi, Mol. Phys. 19 (1970) 553–566.
[13] E.D. Glandening, A.E. Reed, J.E. Carpenter, F. Wienhold, NBO Version 3.1, Gaussian Inc., Pittsburgh, PA, 1992.
[14] A.E. Reed, L.A. Curtiss, F. Wienhold, Chem. Rev. 88 (1988) 899–926.
[15] A.E. Reed, F. Wienhold, Isr. J. Chem. 31 (1991) 277–285.
[16] P. Ludwig, T. Layloff, R.N. Adams, J. Am. Chem. Soc. 86 (1964) 4568–4573.